

1 Compositional shifts associated with major evolutionary transitions in plants

2 Stephen A. Smith, Nathanael Walker-Hale, and C. Tomomi Parins Fukuchi

3

4 **Summary**

- 5 ● Heterogeneity in gene trees, morphological characters, and composition has been  
6 associated with several major clades across the plant tree of life. Here, we examine  
7 heterogeneity in composition across a large transcriptomic dataset of plants in order to  
8 better understand whether locations of shifts in composition are shared across gene  
9 regions and whether directions of shifts within clades are shared across gene regions.
- 10 ● We estimate mixed models of composition for both DNA and amino acids across a  
11 recent large scale transcriptomic dataset for plants.
- 12 ● We find shifts in composition across both DNA and amino acid datasets, with more shifts  
13 detected in DNA. We find that Chlorophytes and lineages within experience the most  
14 shifts. However, many shifts occur at the origins of land, vascular, and seed plants.  
15 While genes in these clades do not typically share the same composition, they tend to  
16 shift in the same direction. We discuss potential causes of these patterns.
- 17 ● Compositional heterogeneity has been highlighted as a potential problem for  
18 phylogenetic analysis, but the variation presented here highlights the need to further  
19 investigate these patterns for the signal of biological processes.

20

21 **Plain language summary**

22 We demonstrate that many nucleotide and amino acid compositional shifts in plants occur at the  
23 origins of major clades and while individual genes do not share the same composition they often  
24 shift in the same direction. We suggest that these patterns warrant further exploration as the  
25 signal of important biological processes during the evolution of plants.

26 **Keywords:** composition, heterogeneity, land plants, evolutionary transitions, transcriptomes

27

## 28 **Introduction**

29 Heterogeneity in the patterns and processes of molecular evolution is common through time and  
30 between lineages. For example, topological conflict between different gene regions has been  
31 demonstrated to be common across the tree of life, reflecting, in part, population processes  
32 including introgression and incomplete lineage sorting (Maddison, 1997; Rokas et al., 2003;  
33 Smith et al., 2015). High rates of morphological change has also been associated with conflict at  
34 several major clades across the plant tree of life (Parins-Fukuchi et al. 2021; Stull et al. 2021).  
35 An additional widely recognized form of heterogeneity is in composition: changes in the  
36 proportion of different states, such as nucleotide bases or Amino Acids (AAs), between lineages  
37 and through time, which emerges from the interplay between mutation, gene conversion, drift  
38 and selection (Eyre-Walker & Hurst, 2001; Lynch, 2007). Compositional differences are also  
39 expressed at the site-level with different protein sites preferring different AAs (Lartillot &  
40 Philippe, 2004; Wang et al., 2008; Le et al., 2008), and genome-wide with different composition  
41 between different regions within the same genome (Lynch, 2007). Different lineages are also  
42 known to favor different synonymous codons, leading to compositional bias at the codon level  
43 (Chen et al., 2004; Plotkin & Kudla, 2011). These differences are tree-heterogeneous and  
44 interactive, so that different sites and loci might experience different compositions in different  
45 lineages at different times.

46 Research intersecting composition and phylogenetics has typically focused on the  
47 impact of heterogeneous composition on error in phylogenetic inference, identifying how clade-  
48 specific biases in nucleotide base composition can produce false groupings of evolutionarily  
49 distant but compositionally similar taxa (Foster, 2004; Cox et al. 2014; Cox, 2018; Sousa et al.,  
50 2020). Another less well-explored avenue is the ability for heterogeneity in composition to  
51 provide a window into the molecular and population processes impacting the genome. A  
52 separate body of research has addressed the role and influence of these processes on

53 genomes in multiple clades (Duret & Galtier, 2009; Glemin et al., 2014; Weber et al., 2014;  
54 Clément et al., 2015; Clément et al., 2017). Mutation pressure is thought to explain some  
55 genomic patterns (Lynch, 2007), such that changes in composition might reflect important shifts  
56 between the balance of mutation and drift, and hence effective population size. GC-Biased  
57 Gene Conversion (gBGC), where GC alleles act as the donor more often than expected during  
58 recombination-associated gene conversion events, also influences genome-wide GC content.  
59 Furthermore, due to gBGC, changes in recombination rate might therefore change compositions  
60 across the tree (Marais et al., 2004; Duret & Galtier, 2009; Muyle et al., 2011; Weber et al.,  
61 2014). Changes in effective population size might drive changes in composition via an increase  
62 in the efficacy of gBGC (Weber et al., 2014). Because gBGC occurs during meiosis, increases  
63 or decreases in generation time could change composition both by changing mutation rate and  
64 changing the number of meiotic, and hence the number of gBGC, events (Romiguier et al.,  
65 2010; Weber et al., 2014).

66 While demographic processes may influence molecular composition, several non-  
67 demographic processes also potentially contribute to compositional change (Clément et al.,  
68 2017; Hershberg & Petrov, 2008). Selection on codon usage for translational accuracy and  
69 efficiency could explain compositional changes (Hershberg & Petrov, 2008; Qiu et al., 2011).  
70 Compositional bias itself may impact codon usage and eventually AA preference (Foster et al.  
71 1997, Singer and Hickey 2000, Knight et al., 2001; Qiu et al., 2011). Bias in the selection for  
72 particular AAs can influence composition (Błażej et al., 2017). Compositionally mediated  
73 changes in codon usage might also influence gene expression (Zhou et al., 2016). In addition to  
74 these microgenomic processes, macrogenomic changes, such as Whole-Genome Duplication  
75 (WGD) and biased retention or loss, could also create dramatic changes in composition  
76 (McGrath et al., 2014; Veleba et al., 2014).

77 In plants, empirical patterns in various clades, such as the GC-richness of Commelinid  
78 monocots, have been described and explained by mutation, selection, and gBGC (Qiu et al.,

79 2011; Serres-Giardi et al., 2012; Glemin et al., 2014; Clément et al., 2015; Clément et al., 2017).  
80 Because shifts in base composition bias can be linked with such crucial evolutionary parameters  
81 as generation time and population size, they may also shed light on major evolutionary  
82 transitions in the plant tree of life.

83         Models of molecular evolution typically consist of two components: relative transition  
84 rates between states, and the composition of those states. State compositions of nucleotides or  
85 AAs are typically modeled at equilibrium, assuming a process that does not vary between sites  
86 or across time (Yang, 2014). These assumptions can be relaxed in several ways including  
87 partitioned models (Lanfear et al., 2012), models that allow the equilibrium composition to vary  
88 across sites (Lartillot & Philippe, 2004; Le et al., 2008), models that vary across the tree (Galtier  
89 & Gouy, 1998; Foster, 2004), or methods that vary substitution models and compositions across  
90 branches (Jayaswal et al., 2011; Zou et al., 2012; Jayaswal et al., 2014). Phylogenetic inference  
91 can be sensitive to composition biases across clades, with conflicting resolutions drawn from  
92 homogeneous vs heterogeneous models. As a result, methods relaxing these assumptions  
93 have been a major focus for phylogenetic inference of ancient nodes across the tree of life  
94 (Sousa et al., 2020; Redmond & McLysaght, 2021; Li et al., 2021). However, if molecular and  
95 population processes are driving the patterns accounted for by heterogeneous phylogenetic  
96 models, these models could be used to detect the signal of changing evolutionary processes  
97 across the tree.

98         Instead of focusing on the resolution of relationships within plants, we concentrate on  
99 examining the extent to which there are compositional shifts across nodes and gene regions.  
100 One shortcoming to the application of phylogenetic methods to the detection of compositional  
101 shifts is that tree-heterogeneous methods typically require the branches of interest to be  
102 specified a priori. Consequently, several efforts have been made to relax this restriction, such as  
103 testing all branches in the tree, or by investigating summary statistics of the substitution  
104 process, or other methods (Blanquart & Lartillot, 2006, 2008; Dutheil et al., 2012). Alternatively,

105 Bayesian MCMC jump methods have been developed that allow for uncertainty in the number  
106 and placement of shifts in composition (Foster, 2004; Gowri-Shankar & Rattray, 2007).  
107 However, computational methods that allow for integrating over the uncertainty of their  
108 placement are too burdensome for large genomic datasets with hundreds of taxa and hundreds  
109 of gene regions. In parallel, research has focused on detecting shifts in the rate of diversification  
110 or phenotypic evolution across the tree (Alfaro et al., 2009; Uyeda & Harmon, 2014; Mitov et al.,  
111 2019). One such class of method uses stepwise model selection with information criteria to  
112 automatically partition the tree into different regimes (Alfaro et al., 2009; Mitov et al., 2019), but  
113 such approaches are not commonly applied to molecular data (but see Dutheil et al., 2012).

114 Here, we extend methods that allow composition to vary across the tree by implementing  
115 an algorithm that detects compositional shifts by comparing models of different dimensions  
116 using information criteria. We apply our method to a large collection of orthologs of coding  
117 regions from across the Viridiplantae clade (Leebens-Mack *et al.*, 2019) and, instead of  
118 targeting the impacts of composition on topological resolution, we focus on identifying  
119 compositional shifts on individual gene regions.

## 120 **Methods**

### 121 *Dataset*

122 We analyzed the nucleotide and AA data from the 1KP transcriptome project data release  
123 available at <https://github.com/smirarab/1kp> (Leebens-Mack *et al.*, 2019) to identify patterns in  
124 compositional heterogeneity across plants. For nucleotide data, we used the “unmasked and  
125 FNA2AA” data and filtered for columns containing at least 10% of data using pxclsq from phyx (-  
126 p 0.1, Brown *et al.*, 2017). We chose these alignments instead of those for which trees were  
127 already inferred in order to include third codon positions for composition analyses. We ran an  
128 analysis to detect compositional shifts in both the nucleotide (the cleaned alignments of all three  
129 codon positions and our inferred trees) and AA data (using the available alignments and trees).  
130 For these alignments, we conducted phylogenetic analyses using IQ-TREE v1.6.6 (Nguyen *et*

131 *al.*, 2015) under the GTR+G model of evolution. For AAs, we used the “masked FAA” data and  
132 the corresponding trees inferred as part of the original study. We analyzed the AA using the JTT  
133 model of evolution. We used a GTR+G model and so there could be phylogenetic error  
134 introduced from violations of homogeneous composition bias. While this may impact some  
135 edges, we have also demonstrated that our method for identifying model shifts is robust to this  
136 (see Supp. Fig. 2).

137         Because of the non-homogeneity of the compositional model, our analysis required  
138 rooted trees. Perfect rooting was not required and would have been prohibitive considering the  
139 variation and non-monophyly of many taxonomic groups in each gene tree (see Supp. Fig. 1). In  
140 order to accommodate this, we rooted using pxrr from phyx, applying the ranked option (-r) with  
141 the following taxa in order (taxon codes from  
142 <https://github.com/smirarab/1kp/blob/master/misc/annotations.csv>): UNBZ, TZJQ, JGGD, HFIK,  
143 YRMA, FOMH, RWXW, FIKG, VYER, LDRY, VRGZ, ULXR, ASZK, JCXF, QLMZ, FSQE,  
144 DBYD, VKVG, BOGT, JQFK, EBWI, FIDQ, QDTV, OGZM, SRSQ, RAPH, LLEN, RFAD, NMAK,  
145 VJED, LXRN, APTP, BAJW, IAYV, IRZA, MJMQ, ROZZ, BAKF. The ranked option searches  
146 through the list of taxa and roots on the first one present.

#### 147 *Detection of compositional heterogeneity*

148 We developed an algorithm to detect locations of shifts in stationary frequencies in state  
149 composition that we describe below (see Figure 1). The method is generalized to any state  
150 model, and so proceeds in the same way for nucleotides or AAs. It requires a rooted tree and  
151 matching alignment as input. First, the method estimates a maximum likelihood root  
152 composition for the entire dataset. Next, the tree is traversed in a postorder fashion (from the  
153 tips to the root), and a maximum likelihood composition is estimated for the subtree subtending  
154 each node, if that subtree contains more than a user-specified minimum number of tips. In this  
155 work, we considered any subtree containing at least 10 tips. Using this composition for the focal  
156 node and subtree, and the root composition for the remainder of the tree, we calculate a

157 likelihood and the Bayesian Information Criterion (BIC: Schwarz, 1978). Once a model for every  
158 eligible subtree has been estimated, we order subtrees by their BIC (i.e., by their relative  
159 improvement in fit over the base model), add them to the model configuration, calculate a new  
160 likelihood and BIC for the whole tree and add the sub-model if the new BIC is lower (i.e., the  
161 model provides a better fit). To improve computational efficiency, we discard models if their BIC  
162 score is greater than the current model by an arbitrary cutoff (we assigned a cutoff of 35). Our  
163 method has been implemented in both Golang (for flexibility) and C (for speed), and the source  
164 code is available at <https://git.sr.ht/~hms/janus> and <https://git.sr.ht/~hms/hringhorni>,  
165 respectively. A diagram is presented in Figure 1 and an empirical example is presented in Supp.  
166 Fig. 3.

### 167 *Accommodating model uncertainty*

168 One common challenge in information criterion (IC) based approaches to model comparison is  
169 their tendency to overfit, sometimes favoring models of higher complexity than the generating  
170 model. Our solution to this tendency was to assess statistical uncertainty in each model shift by  
171 estimating the relative support for the model that includes the shift vs the model without the  
172 shift. We performed these tests using BIC weights ( $wBIC$ ), comparing, for each putative shift,  
173 the BIC of the full model containing all inferred shifts to one dropping each individual model  
174 shift. The strength of support for each inferred shift was thus calculated by calculating the  
175 relative BIC of each candidate model  $i$  (in this case, shift vs no shift):

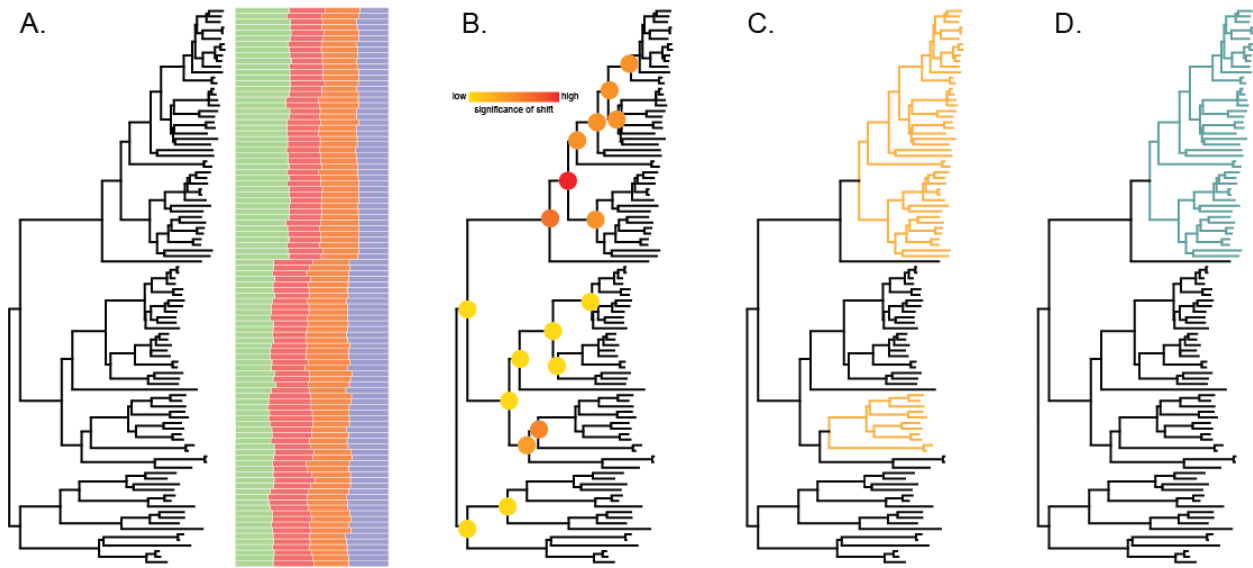
$$176 \quad relBIC_{shift} = e^{(BIC_{shift} - BIC_{no shift}) \times 0.5}$$

177 And assessing support for the shift as the ratio of the ratio of that model over the sum of all  $i$   
178 candidate models:

$$179 \quad wBIC = \frac{relBIC_{no shift}}{(relBIC_{no shift} + relBIC_{shift})}$$

180 This calculation yields an index between 0 and 1, where values closer to 0 indicate weaker  
181 support for the shift, and values closer to 1 indicate stronger support. Using the reasoning that

182 spurious shifts will likely typically be poorly supported, we removed shifts with wBIC support  
183 values below 0.95.



184  
185 Figure 1. A demonstration of the procedure introduced here used on each gene tree. A) shows  
186 a tree and the sequences to the right represented as their composition of DNA. B) is the same  
187 tree with node colors corresponding to the IC values sorted with red being the highest and  
188 yellow being the lowest. C) identifies two clades as having potential shifts with only one  
189 supported after uncertainty analyses (the blue clade in D).

### 190 *Simulations*

191 We conducted several simulations to validate the performance of our algorithm in detecting  
192 model heterogeneity. Phylogenies were simulated under a birth-death model with `phyx` using  
193 the `pxbdsim` command with defaults, except varying the size of the tree between 100 and 250  
194 tips, and root height set to 0.75 with `pxtscale (-r 0.75)` from `phyx`. Nucleotide and AA alignments  
195 were simulated using a simulator `STONE` (<https://git.sr.ht/~hms/stone>) that allows for shifts in  
196 composition across the tree. For nucleotides, we conducted two simulations: one under JC+G  
197 and another GTR+G (both with  $\alpha = 1$  for rate heterogeneity). For AAs we conducted one  
198 simulation under JTT with no rate variation. Each of these simulations had a single randomly



199 positioned compositional shift per tree. Phylogenies were then reconstructed with IQ-TREE  
200 under the GTR+G model of evolution for nucleotide alignments and the JTT+G model for AA  
201 alignments. For each simulation set, we simulated 100 replicates. Alignment lengths were 1000  
202 for nucleotides and 300 and 1000 for Aas.

### 203 *Summarizing compositional heterogeneity*

204 We summarized the results from the empirical analyses in several ways. Directly comparing  
205 model shifts across genes was complicated by extensive gene tree conflict. We compared the  
206 distribution of model shifts by pairwise comparison of tips on the species tree inferred in the  
207 original paper (Leebens-Mack *et al.*, 2019), recording the number of times that two tips were  
208 descended from a node with a shared model, and plotted this in a heatmap on the species tree  
209 (Supp. Fig 4). Secondly, we defined major clades in the species tree, and recorded to which  
210 groups each tip descending a model shift in each gene tree belonged. We counted the number  
211 of tips from each taxonomic group, and further counted the number of tips within those  
212 taxonomic groups which were not included in the model shift (i.e., either the model shift  
213 occurred nested within that group, or those tips were placed polyphyletically in the tree due to  
214 conflict). We manually assessed these mismatches and the position of the model shift on the  
215 gene tree and assigned the shift on the species tree to occur either i) at the node defining a  
216 major clade (assuming mismatching tips are errors), which we summarize as occurring at the  
217 origin of the clade or ii) descending a node defining a major clade, which we summarize as  
218 occurring within the clade. For individual genes, we plotted model shifts on the tree and  
219 changes in parameter estimates between models. To characterize the direction and size of  
220 parameter shifts, we used a Principal Components Analysis where each row was a single  
221 sequence and each column was the frequency of one state for that sequence (i.e., 4 columns  
222 for nucleotides and 20 for Aas). We projected every gene tree onto the same set of axes for the  
223 first two PCs and colored each point (representing a single tip), by the model from which it was  
224 descended. We characterised shift direction and size by projecting fitted model parameters onto

225 the same PC space, and calculating the vector direction and magnitude between the two sets of  
 226 coordinates representing the parent and descendant model.

## 227 **Results**

### 228 *Simulations*

229 Our simulations demonstrate that, given sufficient data (i.e., alignments of sufficient length), our  
 230 method has acceptable false positive and negative rates (Table 1). False positive rates were  
 231 negligible after removing shifts that were poorly supported by BIC. In general, we consider the  
 232 false positive rates to be of more concern than false negatives rates, but the latter were also  
 233 negligible in our simulations. The highest rates of false positives were observed in short (300  
 234 site) AA alignments, which were diminished but not entirely alleviated by taking uncertainty into  
 235 account. False positive rates were generally elevated when tree reconstruction error existed in  
 236 the simulated data. Our simulations also demonstrate that phylogenetic reconstruction error, as  
 237 measured by average RF between the simulated and reconstructed trees, occurred under each  
 238 condition, including with 0 shifts. The RF distance of phylogenies that have one shift with 100  
 239 tips and zero shifts with 100 shifts are not significantly different. Therefore, instead of  
 240 corresponding to the number of shifts or the presence of compositional bias, these errors seem  
 241 to correspond to tree size. We also demonstrate that shifts can be identified correctly even  
 242 when the phylogeny was reconstructed incorrectly (see Supp. Fig 2).

243 Table 1. Results of simulations for both nucleotide (JC/GTR) and amino acid data. Shown are  
 244 false positive (False +) with and without considering uncertainty (unc). We also show results  
 245 considering the correct tree and the tree based on reconstructions (rec). Finally, we present the  
 246 average RF distance between the reconstructed trees and the true tree.

# sh	# tips	N/A	Len	False +	False + unc	False +(rec)	False +(rec) unc	False -	False - unc	False - (rec)	Fals e - (rec) unc	Avg. RF
0	100	N	1000	0/0.02	0/0	0/0.01	0/0	-	-	-	-	9.96/10.88

1	100	N	1000	0/0.04	0/0	0/0.04	0/0.01	0/0	0/0	0/0	0/0	8.76/10.16
2	150	N	1000	0.14/0.13	0.03/0.01	0.09/0.14	0/0.04	0/0.04	0.02/0.04	0/0.05	0.02/0.05	15.0/16.84
2	250	N	1000	0.1/0.14	0.01/0.01	0.1/0.12	0.02/0.03	0.01/0.04	0.03/0.05	0.04/0.06	0.07/0.08	24.8/26.34
0	100	A	300	0	0	0	0	0	0	0	0	14.32
1	100	A	300	0.02	0.01	0.11	0.07	0	0	0.02	0.02	15.9
2	150	A	300	0.03	0	0.18	0.07	0.01	0.01	0.01	0.01	21.34
2	250	A	300	0.02	0	0.19	0.10	0.02	0.03	0.03	0.01	35.6
0	100	A	1000	0	0	0	0	0	0	0	0	4.84
1	100	A	1000	0.01	0	0.03	0.01	0	0	0	0	4.76
2	150	A	1000	0.18	0	0.19	0	0	0	0.01	0.01	6.82
2	250	A	1000	0.22	0	0.22	0.01	0	0	0	0	12.0

247

248 *Phylogenetic patterns of compositional shifts*

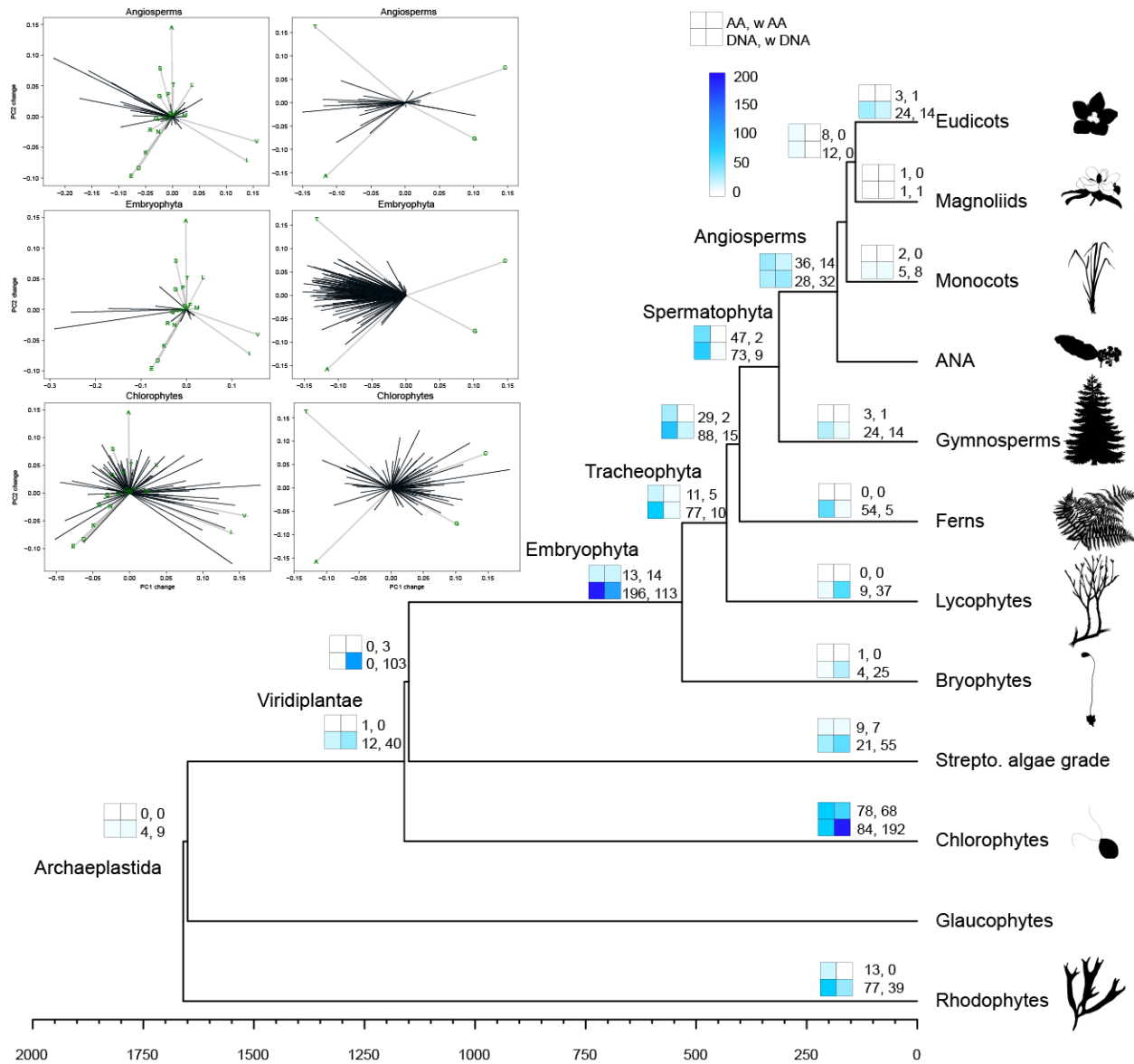
249 We applied our method to a large dataset of orthologs derived from genomes and  
250 transcriptomes across Archaeplastida. As noted in the original study (Leebens-Mack et al.,  
251 2019), the inferred gene trees contained high levels of conflict. For example, 38% of nucleotide  
252 and 32% of AA gene trees contained non-monophyletic seed plants. We searched for  
253 compositional shifts in inferred gene trees from nucleotide and AA data. We detected multiple  
254 shifts in both datasets, with many more shifts detected for nucleotide data (**Figure 2**). The  
255 phylogenetic location of these shifts differed between different trees, and we observed a great  
256 deal of gene tree conflict between the individual orthologs and the species tree, complicating the  
257 localization of shifts. Nevertheless, general patterns did emerge when comparing shift locations  
258 to the species tree (**Figure 2**). Many nucleotide shifts were detected at the Embryophyta node,  
259 corresponding to the origin of land plants, at the Tracheophyta node corresponding to the  
260 evolution of vasculature, at the node uniting ferns and the rest of Spermatophyta, at ferns, at the  
261 Spermatophyta node corresponding to the evolution of seeds, and at the Angiosperm node

262 corresponding to the evolution of flowers. Many nucleotide shifts were also detected at the base  
263 of and within Chlorophytes. By contrast, AA shifts were enriched at the Spermatophyta and  
264 Angiosperm nodes and were similarly common at and within Chlorophytes. Several shifts were  
265 identified within the named clades, such as at or within Eudicots, could not be explored further  
266 because our sampling or the conflict in the gene tree precluded further localization.

#### 267 *Direction of compositional shifts*

268 The direction of compositional shifts (i.e., which state frequencies increased or decreased  
269 between a parent and child model) differed both within and between genes. While specific  
270 compositional values may not be shared by many genes, we noticed a tendency for shifts at  
271 comparable nodes to occur in similar directions (**Figure 4**). The root nodes of angiosperms,  
272 chlorophytes, and embryophytes each displayed many nucleotide composition shifts that were,  
273 for angiosperms and embryophytes, heavily directionally biased towards higher AT (**Figure 2**).  
274 Several nodes displayed similarly biased amino acid compositional shifts. These biased shifts  
275 were highly evident at the origin of Tracheophyta, angiosperms, Zygnematophyceae,  
276 Spermatophyta, Embryophyta, and chlorophytes (Supp. Figs. 5-6).

277 To determine whether patterns in the direction of nucleotide compositional shifts were  
278 related to codon usage bias, we examined codon usage for each model within each gene. We  
279 noted several patterns. Firstly, codon usage was strongly biased within each residue, and there  
280 is a tendency for land plants to feature more AT-rich codons. Additionally, clades nested within  
281 land plants (e.g., Embryophyta, Tracheophyta) tend to be more AT-rich than other clades (e.g.,  
282 Bryophytes). Gymnosperms showed the highest degree of codon usage bias, favoring AT-rich  
283 codons.



284

285 Figure 2. Summarized results for AA and DNA. Inset plots denote vectors of composition shifts

286 for both AA (left) and DNA (right) for Angiosperms, Embryophyta, and Chlorophytes. For the

287 complete set, see Supp Figs. 5 and 6. The black lines in each plot represents a single shift

288 within a single gene. The direction shows the composition shift (e.g., most of the shifts in

289 Embryophyta DNA plots shift to more A and T) and the length of the line shows the strength of

290 the shift. The phylogeny on the right shows shifts detected by clade. There are four boxes at

291 each major clade that correspond to, starting from top left to bottom right, shifts in AA data at

292 that node, shifts in AA data within that node (e.g., because the clade was not monophyletic or

293 because the shift is missing one or more taxa within the clade), shifts in DNA data at that node,  
294 and shifts in DNA data within that node. Colors correspond to the number of shifts. For example,  
295 at Embryophyta, there are 196 DNA shifts at that node and 113 shifts that occur within that node  
296 (missing one or more Embryophyta but not so many as to be considered Tracheophyta or  
297 Bryophytes).

298

299

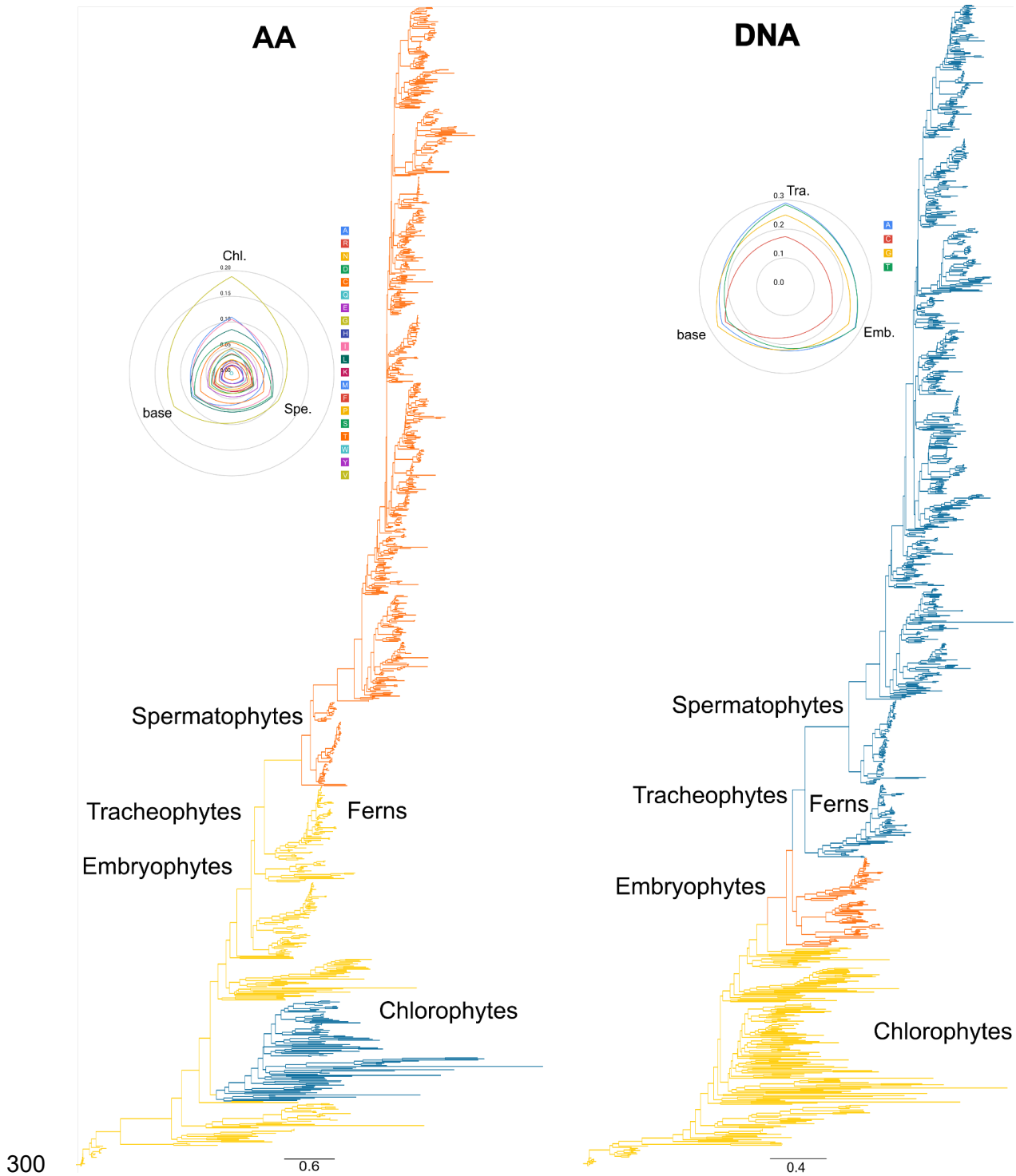
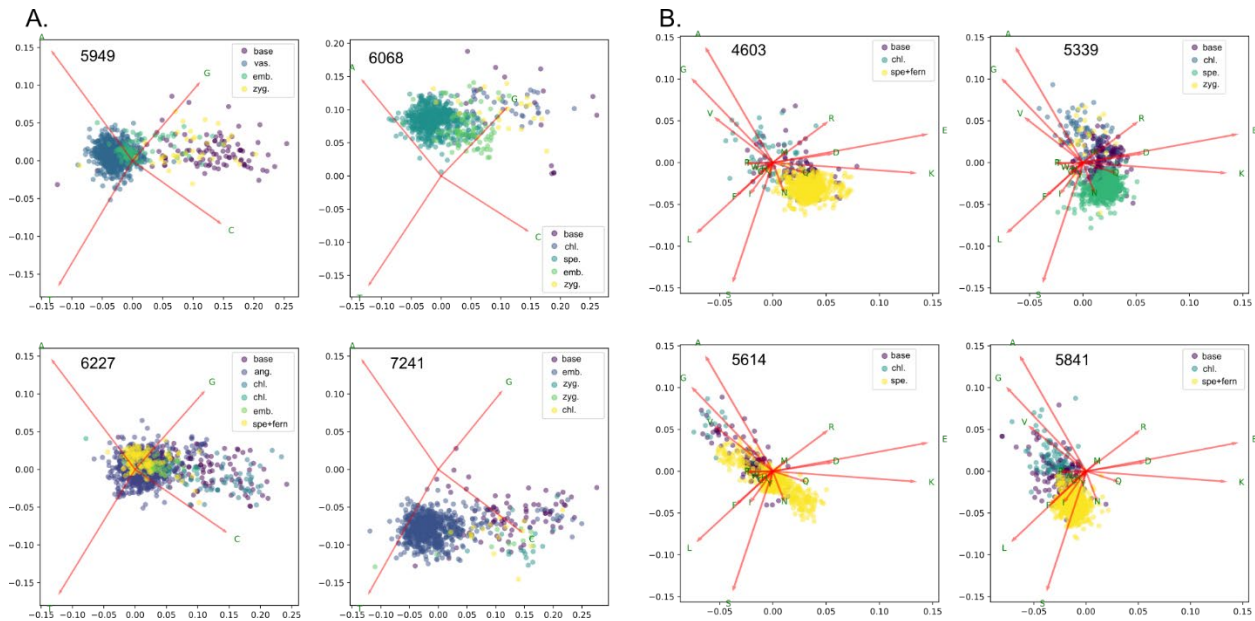


Figure 3. Ortholog 5936 results from both AA and DNA datasets. Colors are meant to identify shifts within the dataset (shared colors between AA and DNA datasets do not denote shared models between AA and DNA results). Base composition model results are presented in radar

304 graphs where lines represent the proportion of the composition in each amino acid or base. For  
305 example, in comparing Tracheophytes and Embryophytes to the base model for DNA, there is  
306 an increase in As and Ts.

307

308



309

310 Figure 4. Principal component analyses of four DNA datasets (A) and four AA datasets (B) with  
311 each point representing one taxon and colors denote shared shifts within the dataset. PC  
312 loadings are based on the entire DNA and AA datasets respectively to allow for easier  
313 interpretation. For 5949, vascular plants and embryophytes have more AT bias than tips sharing  
314 the base model. The same pattern is seen for 6068 for spermatophytes and embryophytes,  
315 angiosperms and spermatophytes in 6227, and embryophytes in 7241. While each is shifting to  
316 more AT, given that these are plotted with the same PC loadings, they are also not converging  
317 on the same space.

318

319 **Discussion**



320 The results of the analyses of the direction of the compositional shifts and the phylogenetic  
321 position of the shifts suggest a common or related causes for these biases for major clades of  
322 land plants. The most notable pattern in this dataset is the tendency for compositional shifts of  
323 Embryophytes, Tracheophytes, and Spermatophytes to be shift to be more AT enriched. Many  
324 of these compositional shifts occur at the origins of these major named clades. The primary  
325 goals of this study are to demonstrate notable patterns of compositional shifts across vascular  
326 plants across gene trees, where previously research has focused on the accuracy of  
327 phylogenetic reconstructions using heterogeneous composition. We discuss potential causes of  
328 this heterogeneity and where certain causes seem plausible based on the analyses here as well  
329 as previous studies. However, additional lines of evidence will be necessary to further narrow  
330 these causes. Nevertheless, the patterns presented here are substantial enough to warrant  
331 further investigation.

332 *Life history.* In our analyses, Chlorophytes tend to have shifts in compositional vectors that vary  
333 widely, some shifts toward elevated GC and some toward elevated AT (Figure 2). In contrast,  
334 land plants, vascular plants, seed plants, and flowering plants, tend to show, when there are  
335 shifts in composition, a tendency towards stronger AT bias. Furthermore, while these genes  
336 show trends towards more AT, there is not a clear lineage specific optimal AT. In other words,  
337 each gene increases in AT but not to the same AT across genes, which reflects documented  
338 intragenomic variation in base compositions (Clement et al., 2017; Glemin et al., 2014). There  
339 may be many potential causes for these patterns, however, one notable difference between  
340 those lineages with shifting AT bias are dramatic changes to life history. Life history has been  
341 demonstrated to have an impact on genome composition. For example, biased gene conversion  
342 can favor the proliferation of GC alleles during meiotic recombination, such that short generation  
343 time could lead to increased GC-richness (Duret & Galtier, 2009; Weber et al., 2014). On the  
344 other hand, mutation tends to be AT biased and lineages with longer generation times are  
345 expected to have higher mutation rates due to more cell divisions and accumulated DNA

346 damage (Lynch, 2007, Bergeron et al. 2023). Population size also plays a compounding role.  
347 Large effective population sizes tend to make natural selection more effective, and in the case  
348 of composition bias this may translate into composition reflecting advantageous selection more  
349 than bias. On the other hand, smaller effective population sizes increase the probability that  
350 mutations will be fixed by drift. Large population sizes and increased generation times are  
351 associated with higher equilibrium GC and faster increases of GC content (Romiguier et al.,  
352 2010), suggesting that reductions in equilibrium GC might reflect shrinking effective population  
353 sizes or increased generation times. Our demographic model suggests that changes at land  
354 plants, vascular plants, seed plants, and angiosperms moved lineages closer to mutation-drift  
355 equilibrium and away from strong natural selection and BGC (Clement et al. 2017). For  
356 Chlorophytes with short generation times and larger population sizes, this may reflect the  
357 variable gene composition. Of note, are the gymnosperms which tend to have higher  
358 composition bias but fewer phylogenetic shifts. Our failure to detect shifts, however, may be due  
359 to lower taxon sampling of the gymnosperms. Alternatively, the slower generation time of  
360 gymnosperms may also play a role, which may have prevented them from reaching  
361 compositional consistency between lineages (Lanfear et al., 2013). This would yield weaker  
362 signals for our methods to detect shifts.

363

364 Our expectations under a model of mutation bias is that populations with slower generation time  
365 and smaller effective population sizes will have lower GC-richness and higher AT-richness at  
366 equilibrium because of AT-biased mutations and a lower rate and a lower efficiency of gBGC.  
367 Our results are consistent with many major changes in traits and life history across the  
368 Viridiplantae being associated with longer generation times and/or reductions in effective  
369 population size. This pattern seems likely to be true of gymnosperms, which are large, long-  
370 lived trees with slow generation times (De La Torre et al. 2017) and our results suggest that it is  
371 true of angiosperms and other lineages.

372

373 *Selection.* In contrast to the demographic explanation above, selection might also drive the  
374 evolution of base composition (Clement et al., 2017; Qiu et al., 2011). Selection on codon usage  
375 could lead to preferred codons for given amino acids which are more GC- or AT-rich, leading to  
376 genome-wide patterns (Hershberg & Petrov, 2008). Because of the bias in codon composition  
377 for certain amino acids, shifts in amino acid preference at particular sites could also produce a  
378 compositional impact (Jobson & Qiu, 2011, but see Wang et al., 2004). In an analysis of extant  
379 plant genomes, Clement et al. (2017) found that the role of selection on codon usage in driving  
380 composition was small relative to BGC. However, we cannot rule out that selection played a role  
381 in generating the patterns we observe here. Moreover, these two explanations are not mutually  
382 exclusive. Selection is expected to be more efficacious in larger populations, so the possible  
383 demographic changes we suggest might interact with selection to produce changes in  
384 equilibrium composition. Further population genetic analysis of extant populations will be  
385 necessary to inform the degree to which these processes interact to shape natural variation in  
386 base composition, including in response to changing population size, generation times, or major  
387 modes of life history (Qiu et al., 2011b). Due to the necessarily coarse nature of our  
388 investigation, it is difficult to comment on how different processes might contribute to the  
389 patterns we observe. Such a distinction is a goal of further modeling efforts (Kostka et al.,  
390 2012), and will undoubtedly be important in more focused studies of single organisms or loci.

391

392 *Population processes, base composition, and gene tree discordance.* Base compositional  
393 biases have been hypothesized to be linked to numerous explicit population processes,  
394 including those outlined above. We suggest that the patterns in base composition shifts that  
395 occur at key nodes in plant phylogeny are likely the result of some combination or subset of  
396 these, and perhaps other, population processes. For example, while we expect life history shifts,  
397 such as lengthening of generation time, to correspond to increases in AT-content, it is important

398 to note that this pattern may also be consistent with myriad other lower-level processes.  
399 Empirically demonstrating a robust link between such broad-scale patterns as those explored  
400 here to specific population processes is notoriously challenging in macroevolutionary studies. In  
401 this study, we were focused on harnessing our new approach on pattern discovery first, while  
402 also considering some possible explanations for these patterns at the population level. Future  
403 work will be needed to more explicitly distinguish between these candidate processes and  
404 understand how each maps to broadly-observable phylogenetic patterns, such as those  
405 reconstructed here. For now, we lack a rigorous understanding of how specific population  
406 processes scale up to phylogenetic patterns and so the first step is to consider as many  
407 candidate processes as possible. A first step may be to identify whether life history shifts are  
408 *statistically* linked with differential patterns in AT-richness. Moving forward, it will become  
409 important to better understand how and whether population processes can be statistically  
410 identified from one another from phylogenetic patterns. Nevertheless, the timing of base  
411 composition shifts that we identify here suggests that major plant clades are reflective of  
412 fundamental biological revolutions, with effects spanning organismal scales from the genome,  
413 through life history, and morphology (Donoghue 2005).

414

415 One increasingly common avenue through which to explore population dynamics such as  
416 incomplete lineage sorting (ILS) and introgression is to explore patterns in gene-tree conflict  
417 (Smith et al. 2015; Smith et al. 2020). We observed substantial topological discordance between  
418 the gene trees analyzed. It has been previously suggested that biases in base composition may  
419 drive error in species tree reconstruction (Cox 2018, Foster 2004). In principle, it is possible that  
420 some proportion of the extensive topological conflict we found in the present dataset was  
421 caused by differential base composition bias across the loci. However, Robinson-Foulds  
422 distances between each gene tree and the species tree were primarily correlated with tree size  
423 with a weak correlation to the number of inferred composition shifts in nucleotides, but a weak

424 negative relationship for AAs, and a great deal of variance unexplained (Table 1 and Supp Figs.  
425 6-7). Here, at most of the major nodes we explored, we found base composition evolution to be  
426 highly biased in its direction, with most loci shifting in a similar direction. As a result, any  
427 reconstruction error caused by base composition issues would likely affect reconstruction at  
428 these nodes roughly uniformly. While we tended to observe a distribution of alternative tree  
429 topologies at each node, previous analyses have found that some of these patterns follow  
430 expectations under population processes such as ILS and introgression (Smith et al. 2020). This  
431 suggests that gene-tree discordance in this dataset is likely caused by a combination of  
432 population processes, such as ILS, and systematic error, perhaps including erroneous ortholog  
433 identification, assembly, and/or contamination. Additionally, we would expect that  
434 compositionally-driven discordance would manifest by uniting clades with disparate  
435 compositions, which our method would then tend to infer as a single, unidirectional shift, as  
436 opposed to the multiple separate shifts we observe here. Therefore, if compositionally-driven  
437 discordance is a major factor in our dataset, it should tend to make our findings conservative by  
438 reconstructing fewer shifts.

439

440 *Phylogenetic resolution.* The simulations conducted here demonstrated that our method can  
441 correctly identify the location of phylogenetic shifts even in the face of reconstruction error.  
442 Nevertheless, the impact of compositional bias on phylogenetic reconstruction has been well  
443 demonstrated. The phylogenetic resolution of several deep nodes differs between genes in the  
444 DNA and amino acid datasets, and some shifts associated with deep nodes are associated with  
445 those alternative resolutions of major clades. For example, in many genes, the Bryophytes are  
446 non-monophyletic and shifts are associated with the nodes surrounding this conflicting  
447 relationship. This has been found previously by Cox et al. (2014). In gene region 6401, the  
448 Bryophytes form a grade with a shift shared by a clade of liverworts and the rest of vascular  
449 plants. The amino acid phylogeny of the same gene has no significant shift in the molecular

450 composition. Other examples include lycopods sister to ferns versus ferns sister to seed plants–  
451 the latter is associated with shifts in molecular evolution 29 times in amino acids and 68 times in  
452 nucleotides. While the analyses presented here are not focused on the phylogenetic resolution  
453 of these major clades, other studies have demonstrated that heterogeneity can alter  
454 phylogenetic reconstruction (CITATIONS). The analyses here underscore the importance of that  
455 consideration in future studies.

456

457 *Data quality.* The datasets we used here present several challenges that may stem from quality-  
458 control issues that are common among large and complex genomic datasets. We note this  
459 problem primarily because as many new genomic and transcriptomic datasets become  
460 available, as in this study, researchers will be tempted to address large scale questions taking  
461 advantage of these enormous datasets. However, caution should continue to be exercised,  
462 because errors in homology or contamination are likely still prevalent, despite researchers' best  
463 efforts. For example, 38% of the nucleotide gene trees and 32% of amino acid gene trees have  
464 non-monophyletic seed plants. This presents several challenges, but primarily, in summarizing  
465 the phylogenetic placement results, we had to accept that there may be outlying taxa that make  
466 strict monophyly difficult to enforce. This conflict, alongside biased per gene taxon sampling, is  
467 probably responsible for our difficulty in recovering some documented patterns of compositional  
468 evolution within angiosperms, such as increases in GC content in Poaceae (Serres-Giardi et al.,  
469 2012). Alternatively, the loci which most strongly express this and analogous patterns may not  
470 have been sampled in this dataset.

471 We highlight this problem not to single out these data or the original analyses as we  
472 recognize that many large-scale datasets inevitably face challenges when cleaning data.  
473 Instead, we want to underscore the importance of homology and orthology analyses in the  
474 construction of single gene alignments and gene trees. While errors like this may not greatly

475 impact species-tree analyses, especially if they are mostly random between gene trees, they  
476 can dramatically limit the utility of these data for other analyses.

477

#### 478 **Acknowledgements**

479 We would like to acknowledge the importance of several discussions with colleagues including  
480 James Pease, Greg Stull, Jeremy Beaulieu and the Smith lab group. SAS was supported by a  
481 MICDE discovery grant and NSF 1938969 and 1917146. NWH was supported by the Woolf  
482 Fisher Trust.

483

484 **Author Contribution:** SAS, CPF, and NWH contributed to the conception, programming, and  
485 writing of the manuscript.

486

#### 487 **Data Availability**

488 The alignments for both DNA and amino acid datasets are available through the resources of  
489 the original data release paper. The gene trees for DNA were generated as part of this study  
490 and are available from DataDryad. The code is available through github and sourcehut linked  
491 above.

492

#### 493 **References**

494 **Alfaro ME, Santini F, Brock C, Alamillo H, Dornburg A, Rabosky DL, Carnevale G, Harmon**

495 **LJ. 2009.** [Nine exceptional radiations plus high turnover explain species diversity in jawed](#)

496 [vertebrates](#). *Proceedings of the National Academy of Sciences* **106**: 13410–13414.

497 **Bergeron LA, Besenbacher S, Zheng J, Li P, Bertelsen MF, Quintard B, Hoffman JI, Li Z,**

498 **St Leger J, Shao C, Stiller J, Gilbert MTP, Schierup MH, Zhang G. 2023.** Evolution of the

499 germline mutation rate across vertebrates. *Nature* <https://doi.org/10.1038/s41586-023-05752-y>

- 500 **Blanquart S, Lartillot N. 2006.** [A bayesian compound stochastic process for modeling](#)  
501 [nonstationary and nonhomogeneous sequence evolution](#). *Molecular Biology and Evolution* **23**:  
502 2058–2071.
- 503 **Blanquart S, Lartillot N. 2008.** [A site- and time-heterogeneous model of amino acid](#)  
504 [replacement](#). *Molecular Biology and Evolution* **25**: 842–858.
- 505 **Błażej P, Mackiewicz D, Wnętrzak M, Mackiewicz P. 2017.** [The impact of selection at the](#)  
506 [amino acid level on the usage of synonymous codons](#). *G3 GenesGenomesGenetics* **7**: 967–  
507 981.
- 508 **Cannon CH, Piovesan G, Munne-Bosch S. 2022.** Old and ancient trees are life history lottery  
509 winners and vital evolutionary resources for long-term adaptive capacity. *Nature Plants* **8**: 136-  
510 145
- 511 **Chen SL, Lee W, Hottes AK, Shapiro L, McAdams HH. 2004.** [Codon usage between](#)  
512 [genomes is constrained by genome-wide mutational processes](#). *Proceedings of the National*  
513 *Academy of Sciences* **101**: 3480–3485.
- 514 **Clément Y, Fustier M-A, Nabholz B, Glémin S. 2015.** [The bimodal distribution of genic GC](#)  
515 [content is ancestral to monocot species](#). *Genome Biology and Evolution* **7**: 336–348.
- 516 **Clément Y, Sarah G, Holtz Y, Homa F, Pointet S, Contreras S, Nabholz B, Sabot F, Sauné**  
517 **L, Ardisson M, et al. 2017.** [Evolutionary forces affecting synonymous variations in plant](#)  
518 [genomes](#). *PLOS Genetics* **13**: e1006799.
- 519 **Cox CJ, Li B, Foster PG, Embley M, Civan P. 2014.** Conflicting phylogenies for early land  
520 plants are caused by composition biases among synonymous substitutions. *Systematic Biology*  
521 **63**:272-279.
- 522 **Cox CJ. 2018.** [Land plant molecular phylogenetics: A review with comments on evaluating](#)  
523 [incongruence among phylogenies](#). *Critical Reviews in Plant Sciences* **37**: 113–127.



- 524 **De La Torre A, Li Z, Van de Peer Y, Ingvarsson PK. 2017.** [Contrasting Rates of Molecular](#)  
525 [Evolution and Patterns of Selection among Gymnosperms and Flowering Plants.](#) *Molecular*  
526 *Biology and Evolution* **34**: 1363-1377.
- 527 **Donoghue MJ. 2005.** Key innovations, convergence, and success: Macroevolutionary lessons  
528 from plant phylogeny. *Paleobiology*. 31:77-93.
- 529 **Duret L, Galtier N. 2009.** [Biased gene conversion and the evolution of mammalian genomic](#)  
530 [landscapes.](#) *Annual Review of Genomics and Human Genetics* **10**: 285–311.
- 531 **Dutheil JY, Galtier N, Romiguier J, Douzery EJP, Ranwez V, Boussau B. 2012.** [Efficient](#)  
532 [selection of branch-specific models of sequence evolution.](#) *Molecular Biology and Evolution* **29**:  
533 1861–1874.
- 534 **Eyre-Walker A, Hurst LD. 2001.** [The evolution of isochores.](#) *Nature Reviews Genetics* **2**: 549–  
535 555.
- 536 **Foster PG, Jermini LS, Hickey DA. 1997.** Nucleotide composition bias affects amino acid  
537 content in proteins coded by animal mitochondria. *J. Mol Evol* **44**:282-288.
- 538 **Foster PG. 2004.** [Modeling compositional heterogeneity.](#) *Systematic Biology* **53**: 485–495.
- 539 **Galtier N, Gouy M. 1998.** [Inferring pattern and process: Maximum-likelihood implementation of](#)  
540 [a nonhomogeneous model of DNA sequence evolution for phylogenetic analysis.](#) *Molecular*  
541 *Biology and Evolution* **15**: 871–879.
- 542 **Glémin S, Clément Y, David J, Ressayre A. 2014.** GC content evolution in coding regions of  
543 angiosperm genomes: a unifying hypothesis. *Trends in Genetics* **30**: 263–270.
- 544 **Gowri-Shankar V, Rattray M. 2007.** [A reversible jump method for bayesian phylogenetic](#)  
545 [inference with a nonhomogeneous substitution model.](#) *Molecular Biology and Evolution* **24**:  
546 1286–1299.
- 547 **Hershberg R, Petrov DA. 2008.** Selection on Codon Bias. *Ann. Rev. Gen.* **42**: 287-299.
- 548 **Jayaswal V, Ababneh F, Jermini LS, Robinson J. 2011.** [Reducing model complexity of the](#)  
549 [general markov model of evolution.](#) *Molecular Biology and Evolution* **28**: 3045–3059.

- 550 **Jayaswal V, Wong TKF, Robinson J, Poladian L, Jermini LS. 2014.** [Mixture models of](#)  
551 [nucleotide sequence evolution that account for heterogeneity in the substitution process across](#)  
552 [sites and across lineages](#). *Systematic Biology* **63**: 726–742.
- 553 **Jiao Y, Wickett NJ, Ayyampalayam S, Chanderbali AS, Landherr L, Ralph PE, Tomsho LP,**  
554 **Hu Y, Liang H, Soltis PS, et al. 2011.** Ancestral polyploidy in seed plants and angiosperms.  
555 *Nature* **473**: 97–100.
- 556 **Jobson RW, Qiu Y-L. 2011.** Amino Acid Compositional Shifts During Streptophyte Transitions  
557 to Terrestrial Habitats. *Journal of Molecular Evolution* **72**: 204–214.
- 558 **Knight RD, Freeland SJ, Landweber LF. 2001.** [A simple model based on mutation and](#)  
559 [selection explains trends in codon and amino-acid usage and GC composition within and across](#)  
560 [genomes](#). *Genome Biology* **2**: research0010.1.
- 561 **Kostka D, Hubisz MJ, Siepel A, Pollard KS. 2012.** The Role of GC-Biased Gene Conversion  
562 in Shaping the Fastest Evolving Regions of the Human Genome. *Molecular Biology and*  
563 *Evolution* **29**: 1047–1057.
- 564 **Lanfear R, Calcott B, Ho SYW, Guindon S. 2012.** [PartitionFinder: Combined selection of](#)  
565 [partitioning schemes and substitution models for phylogenetic analyses](#). *Molecular Biology and*  
566 *Evolution* **29**: 1695–1701.
- 567 **Lanfear R, Ho SYW, Jonathan Davies T, Moles AT, Aarssen L, Swenson NG, Warman L,**  
568 **Zanne AE, Allen AP. 2013.** Taller plants have lower rates of molecular evolution. *Nature*  
569 *Communications* **4**: 1879.
- 570 **Lartillot N, Philippe H. 2004.** [A bayesian mixture model for across-site heterogeneities in the](#)  
571 [amino-acid replacement process](#). *Molecular Biology and Evolution* **21**: 1095–1109.
- 572 **Le SQ, Lartillot N, Gascuel O. 2008.** [Phylogenetic mixture models for proteins](#). *Philosophical*  
573 *Transactions of the Royal Society B: Biological Sciences* **363**: 3965–3976.

574 **Leebens-Mack JH, Barker MS, Carpenter EJ, Deyholos MK, Gitzendanner MA, Graham**  
575 **SW, Grosse I, Li Z, Melkonian M, Mirarab S, et al. 2019.** One thousand plant transcriptomes  
576 and the phylogenomics of green plants. *Nature* **574**: 679–685.

577 **Li Y, Shen X-X, Evans B, Dunn CW, Rokas A. 2021.** [Rooting the animal tree of life](#). *Molecular*  
578 *Biology and Evolution* **38**: 4322–4333.

579 **Lynch M. 2007.** *The origins of genome architecture*. Sunderland, MA: Sinauer Associates.

580 **McGrath CL, Gout J-F, Doak TG, Yanagi A, Lynch M. 2014.** Insights into Three Whole-  
581 Genome Duplications Gleaned from the *Paramecium caudatum* Genome Sequence. *Genetics*  
582 **197**: 1417–1428.

583 **Maddison WP. 1997.** [Gene trees in species trees](#). *Systematic Biology* **46**: 523–536.

584 **Marais G, Charlesworth B, Wright SI. 2004.** [Recombination and base composition: The case](#)  
585 [of the highly self-fertilizing plant arabidopsis thaliana](#). *Genome Biology* **5**: R45.

586 **Mitov V, Bartoszek K, Stadler T. 2019.** [Automatic generation of evolutionary hypotheses using](#)  
587 [mixed gaussian phylogenetic models](#). *Proceedings of the National Academy of Sciences* **116**:  
588 16921–16926.

589 **Mugal CF, Weber CC, Ellegren H. 2015.** GC-biased gene conversion links the recombination  
590 landscape and demography to genomic base composition. *BioEssays* **37**: 1317–1326.

591 **Muyle A, Serres-Giardi L, Ressayre A, Escobar J, Glémin S. 2011.** [GC-biased gene](#)  
592 [conversion and selection affect GC content in the oryza genus \(rice\)](#). *Molecular Biology and*  
593 *Evolution* **28**: 2695–2706.

594 **Parins-Fukuchi CT, Stull GW, Smith SA. 2021.** Phylogenomic conflict coincides with rapid  
595 morphological innovation. *PNAS* **118** (19) e2023058118.

596 **Plotkin JB, Kudla G. 2011.** [Synonymous but not the same: The causes and consequences of](#)  
597 [codon bias](#). *Nature Reviews Genetics* **12**: 32–42.

- 598 **Qiu S, Zeng K, Slotte T, Wright S, Charlesworth D. 2011.** Reduced Efficacy of Natural  
599 Selection on Codon Usage Bias in Selfing Arabidopsis and Capsella Species. *Genome Biology*  
600 *and Evolution* **3**:868-880.
- 601 **Qiu S, Bergero R, Zeng K, Charlesworth D. 2011.** [Patterns of codon usage bias in silene](#)  
602 [latifolia](#). *Molecular Biology and Evolution* **28**: 771–780.
- 603 **Redmond AK, McLysaght A. 2021.** [Evidence for sponges as sister to all other animals from](#)  
604 [partitioned phylogenomics with mixture models and recoding](#). *Nature Communications* **12**: 1783.
- 605 **Rokas A, Williams BL, King N, Carroll SB. 2003.** [Genome-scale approaches to resolving](#)  
606 [incongruence in molecular phylogenies](#). *Nature* **425**: 798–804.
- 607 **Romiguier J, Ranwez V, Douzery EJP, Galtier N. 2010.** [Contrasting GC-content dynamics](#)  
608 [across 33 mammalian genomes: Relationship with life-history traits and chromosome sizes](#).  
609 *Genome Research* **20**: 1001–1009.
- 610 **Serres-Giardi L, Belkhir K, David J, Glémin S. 2012.** Patterns and Evolution of Nucleotide  
611 Landscapes in Seed Plants. *The Plant Cell* **24**: 1379–1397.
- 612 **Singer GAC, Hickey DA. 2000.** Nucleotide bias causes a genomewide bias in the amino acid  
613 composition of proteins. *Molecular Biology and Evolution* **17**:1581-1588.
- 614 **Smith SA, Moore MJ, Brown JW, Yang Y. 2015.** [Analysis of phylogenomic datasets reveals](#)  
615 [conflict, concordance, and gene duplications with examples from animals and plants](#). *BMC*  
616 *Evolutionary Biology* **15**: 150.
- 617 **Smith SA, Walker-Hale N, Walker JF, Brown JW. 2020.** Phylogenetic Conflicts, Combinability,  
618 and Deep Phylogenomics in Plants. *Systematic Biology* **69**: 579-592.
- 619 **Sousa F, Civián P, Foster PG, Cox CJ. 2020.** [The chloroplast land plant phylogeny: Analyses](#)  
620 [employing better-fitting tree- and site-heterogeneous composition models](#). *Frontiers in Plant*  
621 *Science* **11**.
- 622 **Stull GW, Qu XJ, Parins-Fukuchi CT, Yang YY, Yang JB, Yang ZY, Hong Ma YH, Soltis PS,**  
623 **Soltis DE, Li D, Smith SA, Yi TS. 2021.** Gene duplications and phylogenomic conflict underlie

624 major pulses of phenotypic evolution in gymnosperms. *Nat. Plants* 7, 1015–1025.  
625 <https://doi.org/10.1038/s41477-021-00964-4>

626 **Uyeda JC, Harmon LJ. 2014.** [A novel bayesian method for inferring and interpreting the](#)  
627 [dynamics of adaptive landscapes from phylogenetic comparative data.](#) *Systematic Biology* **63**:  
628 902–918.

629 **Veleba A, Bureš P, Adamec L, Šmarda P, Lipnerová I, Horová L. 2014.** Genome size and  
630 genomic GC content evolution in the miniature genome-sized family Lentibulariaceae. *New*  
631 *Phytologist* **203**: 22–28.

632 **Wang H-C, Li K, Susko E, Roger AJ. 2008.** [A class frequency mixture model that adjusts for](#)  
633 [site-specific amino acid frequencies and improves inference of protein phylogeny.](#) *BMC*  
634 *Evolutionary Biology* **8**: 331.

635 **Wang H, Singer GAC, Hickey DA. 2004.** Mutational Bias Affects Protein Evolution in Flowering  
636 Plants. *Molecular Biology and Evolution* **21**: 90–96.

637 **Weber CC, Boussau B, Romiguier J, Jarvis ED, Ellegren H. 2014.** [Evidence for GC-biased](#)  
638 [gene conversion as a driver of between-lineage differences in avian base composition.](#) *Genome*  
639 *Biology* **15**: 549.

640 **Yang Z. 2014.** *Molecular evolution: A statistical approach.* OUP Oxford.

641 **Zhou Z, Dang Y, Zhou M, Li L, Yu C, Fu J, Chen S, Liu Y. 2016.** [Codon usage is an important](#)  
642 [determinant of gene expression levels largely through its effects on transcription.](#) *Proceedings*  
643 *of the National Academy of Sciences* **113**: E6117–E6125.

644 **Zou L, Susko E, Field C, Roger AJ. 2012.** [Fitting nonstationary general-time-reversible models](#)  
645 [to obtain edge-lengths and frequencies for the barry–hartigan model.](#) *Systematic Biology* **61**:  
646 927–940.  
647